ISSN 1590-8844
International Journal of Mechanics and Control, Vol. 16, No. 02, 2015

EFFECTS OF EARTHQUAKE MOTION ON MECHANISM OPERATION: AN EXPERIMENTAL APPROACH

Özgün Selvi[1] Marco Ceccarelli[2] Erman B. Aytar[3]

[1] Cankaya University, Ankara, Turkey

[2] LARM, Laboratory of Robotics and Mechatronics, University of Cassino and South Latium, Italy

[3] Izmir Institute of Technology, Izmir, Turkey

ABSTRACT

This paper presents an experimental characterization of the effects of earthquakes on the operation of mechanical systems with the help of CaPaMan (Cassino Parallel Manipulator), which is a 3 DOF robot that can fairly well simulate 3D earthquake motion. The sensitivity of operation characteristics of machinery to earthquake disturbance is identified and characterized through experimental tests. Experimental tests have been carried out by using a slider-crank linkage, a small car model, and LARM Hand as test-bed mechanisms that have been sensored with proper acceleration or force sensors. Results are reported and discussed to describe the effects of earthquake motion on the characteristics of mechanism operation as a service application of the robotic CaPaMan system.

Keywords: Experimental mechanics; Simulation; Mechanisms; Earthquake effects

1 INTRODUCTION

For investigating the earthquake characteristics and earthquake-resistant constructions, earthquake simulators are commonly used for experimental tests in the field of Civil Engineering. For dynamic testing of structures subjected to earthquake accelerations and for experimenting effects on structures small scale uni-axial servo-hydraulic seismic simulators have become popular, [1, 2]. A number of new large-scale seismic simulator facilities have recently been presented as in [3, 4, 5], and some exceptional simulators, like for example in [6], are also made for outdoor. The case of 6 DoF motion simulator is also presented for shaking tables in [7]. It is important to have earthquake simulators that can reproduce earthquakes with main real characteristics. Generally, most of the earthquake simulators are shaking tables, which are actuated by hydraulic actuators that are fixed on the base. High payload capacity, high motion speeds, and high accelerations are the main characteristics of shaking tables, but they refer to seismic translational motions only.

A new earthquake simulator is a suitable service application of CaPaMan which can simulate not only translational motion but also 3-D waving motions of earthquakes. Performances and suitable formulation for the operation of CaPaMan as earthquake simulator have been presented by theoretical investigations and experimental validations in [8-11]. In fact, CaPaMan can be operated fairly easily by giving suitable input motion to obtain any kind of earthquake in terms of magnitude, frequency and duration.

A novel field of interest can be recognized in investigating the effects of earthquake motion on the operation of machinery. Although vibrations are well known as affecting the machinery operation, the specific effects of earthquake actions on machinery characteristics are not yet fully explored. In previous works [12] the effects of earthquakes on mechanism operation are shown with first experiments on a slider-crank mechanism and a robotic hand.

In this paper the effects of earthquake on the operation of mechanical systems have been investigated experimentally by an analysis and reproduction of an earthquake motion

Contact author: Özgün Selvi[1], Marco Ceccarelli[2]

[1] Cankaya University, Ankara, Turkey.
E-mail: ozgunselvi@cankaya.edu.tr

[2] LARM, Laboratory of Robotics and Mechatronics, University of Cassino and South Latium, Italy
E-mail: ceccarelli@unicas.it

disturbing machine operation. This paper illustrates a specific activity that has been focused in determining experimentally the effects of earthquake motion on mechanism operation by looking at the changes in the motion (acceleration) or force outputs of the mechanisms. Experimental tests have been carried out by using a slider-crank linkage with servo motor, a small car model, and LARM Hand as test-bed mechanisms with acceleration or force sensors in a service application of CaPaMan system.

2 MOTION CHARACTERISTICS OF EARTHQUAKES

A sudden and sometimes catastrophic movement of a part of the surface of the Earth is called an earthquake when it results from a dynamic release of elastic strain energy with seismic waves. Large earthquakes can cause serious destruction and massive loss of life through a variety of damages such as fault rupture, vibratory ground motion, inundation, permanent ground failures, and fire or a release of hazardous materials, and even buildings/constructions collapses and vehicles/machinery operation crashes. Ground motion is the dominant and most widespread cause of damages, as stressed in [13].

In general an earthquake has three phases, namely an initial phase, which corresponds to the beginning of the seismic motion, an intermediate phase where maximum acceleration peaks and displacements occur, and a final phase representing the end of the earthquake. Main characteristics of an earthquake are frequency, amplitude, and acceleration magnitude, because the resonance of a system is determined by frequency value, duration of the stress action due to a seismic motion, amplitude and acceleration magnitude of an earthquake excitation.

A seismic motion is characterized by the period of a seismic cycle and characteristic length for each seismic wave. As shown in Fig.1 [13], main types of seismic waves can be considered the compression expansion waves P, transversal waves S, and superficial waves M, when referring to the spread speed and terrain movements. S waves are transversal waves and their usual period is between 0.5 and 1 second. The P waves spread through a spring-like-motion with a typical period between 0.1 and 0.2 second. Both P and S waves occur close to the epicenter. Unlike P and S waves, M waves occur on the surface of the terrain at a considerable distance from the epicenter of the earthquake and usually they have a period from 20 second to 1 minute.

In Figure 1.c) main differences among the seismic waves are represented in terms of acceleration magnitude and characteristic period of oscillating motion, which is responsible of a periodical excitation of structures that can be damaged when resonance situation occurs.

Usually, critical resonant motion is analyzed in terms of translational seismic components, but even angular motion can strongly contribute to the resonant excitation. Thus, unlike most of the simulators that do not consider the 3D motion of the terrain due to earthquake, in this paper 3D motion capability of CaPaMan parallel manipulator has been used to simulate earthquake motion with its full motion effects. Thus, an earthquake simulator has been arranged with CaPaMan as service system for experiencing the variety of seismic motions and their effect on mechanism operation.

3 OPERATION OF MECHANISMS

As mentioned in terminology of IFToMM [14] a machine is a "mechanical system that performs a specific task, such as the forming of material, and the transference and transformation of motion and force". Similarly a mechanism is defined as a "constrained system of bodies designed to convert motions of, and forces on, one or several bodies into motions of, and forces on, the remaining bodies". Mechanisms, which can be considered the core parts for machines, are combination of gears, cams, linkages, springs, and other mechanical parts [15, 16].

Properties of mechanisms operation can be characterized by input-output relationships, motion performance of task unit, energy efficiency, and so on. In a design process a task goal of the can be classified as function generation, point guidance, and body guidance [15, 16]. Function generation is the coordination of positions of the input and output links, in which the output members need to rotate, oscillate or reciprocate according to a specified function of time or input motion. Path generation is the design of mechanism for guiding a coupler point along a described path. Rigid body guidance is the problem of translation and/or orientation of a rigid body from one position to another.

Machinery operations are usually worked out to perform motions and actions with the task performance that are related to the machinery aim and also interaction with users and environments.

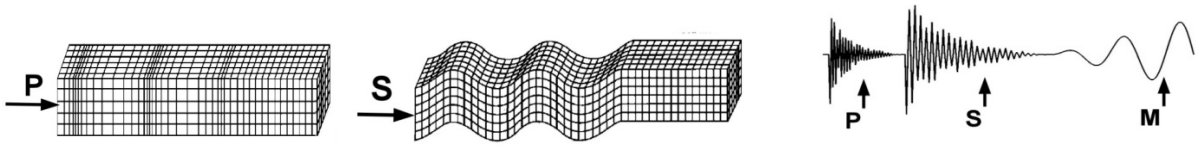

a) b) c)

Figure 1 Basic characteristics of seismic waves [13]:
a) compression and expansion waves; b) transversal waves; c) types of seismograms.

A machinery aim can be in general described by mechanical properties whose performance merits can be expressed in term of motion characteristics and transmission actions with efficiency features both from kinematical and energy viewpoints. Machinery interactions can be understood as related to the effects toward the surrounding environment and mainly as from the viewpoint of human-machine interactions. Those last features will include issues on comfort and safety that can make strong constraints to machinery operations with limited range of operation feasible characteristics. Thus, machinery operations can be described and characterized by performance indices which can be formulated for general but specific aspects that permit both design procedures towards optimal solutions and experimental control/monitoring of successful operation. Special attention is today addressed to safety as interaction with human users, even when using a machine under critical risky situations which can be characterized by impact, high accelerations or changed operation outputs. Even efficiency in force transmission and energy consumption are of great importance in modern machinery.

In general the effects of earthquakes are neglected during machine design. The difficulty to determine the effects of earthquakes is due to different types of totally random waves caused by them, as mentioned in section 2. An illustrative example of earthquake influence on machinery operation can be given as referring to the running of a train. Input for trains is the action of actuators for wheel motion, task for the train is the body guidance of the train, and the output is a stable motion with the features of comfort, safety, efficiency and reliability. A general disturbance of train operation is related to vibrations which effect also comfort of passengers. Comfort in train task is felt by human users mainly in terms of acceleration of the train cars. This task efficiency of cars motion is a result from the transmission of motions and forces from the mechanism for the wheel actuation and car guidance during train run. Those characteristics are demanded in more robust outputs in faster trains. Motion disturbances can produce not only uncomfortable operation, but even risks of disasters in train run, as it can occur in the case of earthquakes.

In order to define a motion of a mechanism it is essential for the mechanism to have a fixed frame which is usually ground. In the event of an earthquake the fixed frame starts to move and apply unexpected random forces to the mechanism so that it may produce changes in the mechanisms outputs. These unexpected changes should be investigated to give useful feedbacks for the design and operation of machines that can work properly even under earthquake disturbances.

3.1 AN EXAMPLE WITH A SLIDER CRANK MECHANISM

For converting rotary motion into alternating linear motion the mostly used mechanism is the slider-crank mechanism shown in Figure 2.a). A slider-crank mechanism consists of four bodies that are linked with three revolute joints and one prismatic joint. Four different mechanisms or inversions of this kinematic chain are possible as depending on which body is grounded, namely the crank, connecting link, sliding link or slot link. One of the inversions of slider crank mechanism is used in internal combustion engines (automobiles, trucks, and small engines). A wide use of these machines makes the slider-crank mechanism the most used mechanism in the world.

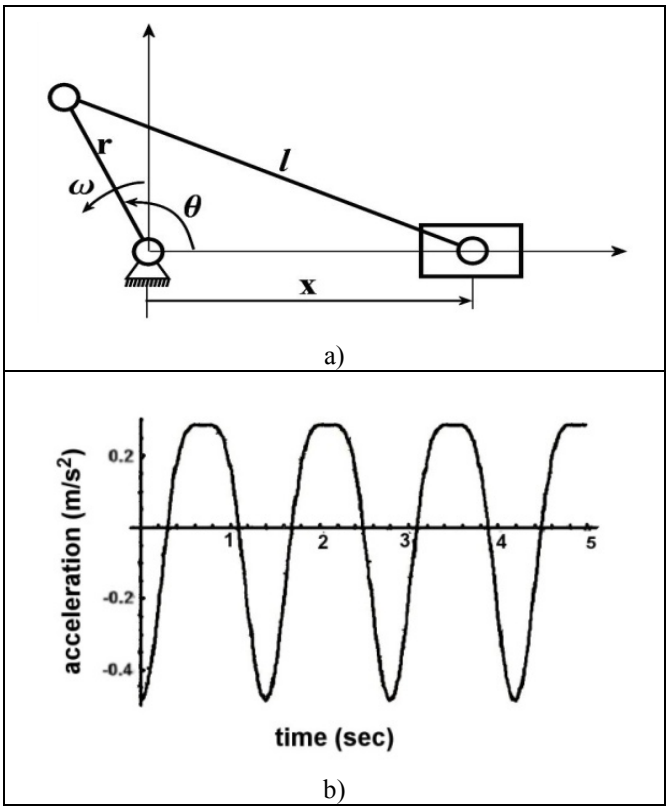

Figure 2 A test-bed slider-crank mechanism:
a) kinematic parameters; b) slider accelerations with stationary frame and input motion at 43 rpm.

In Figure 2.a) kinematic parameters of slider crank are shown, acceleration equation as output of the slider can be calculated from the acceleration equation of the slider with respect to input rotation as,

$$\ddot{x}=-r\alpha\left(\sin\theta+\frac{r\sin 2\theta}{2l}\right)-r\omega^2\left(\cos\theta+\frac{r\cos 2\theta}{l}\right) \qquad (1)$$

A numerical computation is shown in Figure 2.b) which shows a nearly harmonic motion for slider acceleration.

Expected influence during a seismic disturbance can give changes in the shape and magnitude of the slider acceleration with significant alteration of the task motion behaviour. But Eq.(1) gives indication of which parameter can be affected or can be used for limiting this effects.

4 EXPERIMENTAL SETUP WITH CAPAMAN AS EARTHQUAKE SIMULATOR

The here-in test-bed prototype for earthquake simulator shown in Figure 3 consists of a service application of CaPaMan (Cassino Parallel Manipulator) when equipped with acceleration sensors, a controller for seismic motion reproduction, and an acquisition board that is connected to a computer. Data acquisition is used to monitor accelerations that occur along the axes of a reference system that is fixed on the mobile platform [8, 9].

Since the minimum number of accelerometers that are needed to describe velocity and acceleration of a 3D motion of a rigid body is twelve when properly located [17], CaPaMan has been equipped with four of three-axis accelerometers are installed with a symmetrical distribution. The four three-axis accelerometers are located on the below surface of the CaPaMan platform with positions that are indicated in Figure 4. The control system scheme layout for CaPaMan manipulator is shown in Figure 5. Motors signals for simulating an earthquake are sent from a servo motor controller (Scorbot-ER V) by using the ACL programming language for the formulated closed-form direct kinematics of CaPaMan. The motors move the mobile platform as a seismic testing frame and the acceleration information of the mobile platform is processed through the NI-DAQ 6210 and then visualized with the LabView software.

A suitable Virtual Instrument has been developed in LabView environment to manage the signals coming from sensors. The measured acceleration data from the accelerometers are used to compute the acceleration of the center point H of the moving plate and plate angular velocity, beside monitoring the acceleration of the simulated seismic motion.

Figure 3 An experimental setup of CaPaMan as earthquake simulator at LARM with a slider-crank mechanism.

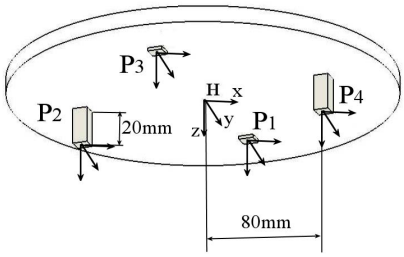

a)

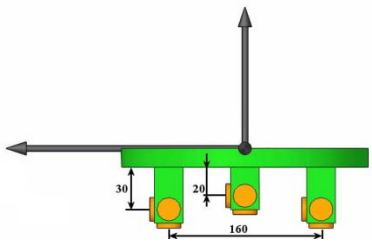

b)

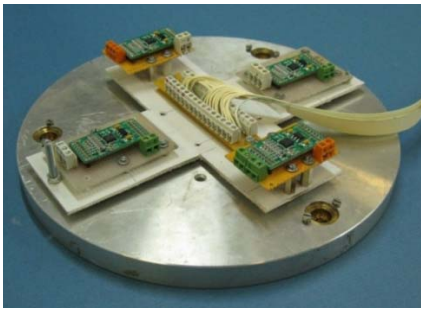

c)

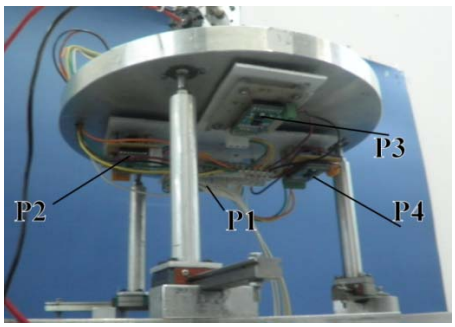

d)

Figure 4 Sensored CaPaMan platform with accelerometers:
a) a scheme, b) sensor locations, c) sensor installation, d) test lay-out.

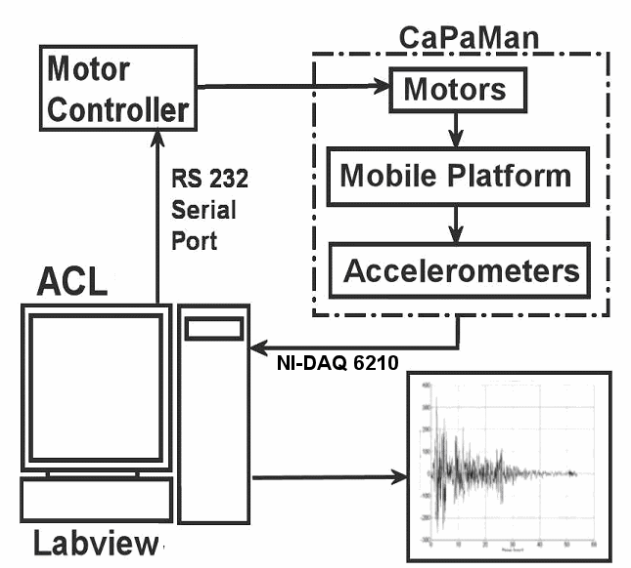

Figure 5 Control system layout for CaPaMan as earthquake simulator.

Two types of earthquakes are simulated for a characterization of earthquake effects on mechanism operation. Characteristic phases of the simulated earthquakes are given in Table I and a reference earthquake that is shown in Figure 6 is used for defining parameters of earthquake characteristics. Type 1 and 2 in Table I refer to typical earthquakes with different time parameters and frequency of motion excitation, as from the mort recurrent events.

Typical values of measured accelerations in simulated earthquake of type 1 are shown in Figure 7.

In order to calculate accelerations and velocities characterizing the seismic effects in an experimental set up an analysis of rigid body motion must be properly formulated as we may suggest in the following. The acceleration of a point P in a rigid body in a position with **r** with respect to a reference frame can be expressed by [17],

$$\mathbf{a}_P = \mathbf{a}_B + \boldsymbol{\alpha}_B \times \mathbf{r} + \boldsymbol{\omega}_B \times (\boldsymbol{\omega}_B \times \mathbf{r}) \tag{2}$$

where acceleration $\mathbf{a}_B$, angular velocity $\boldsymbol{\omega}_B$ and angular acceleration $\boldsymbol{\alpha}_B$ refer to the relative movement of the rigid body frame O_B with respect to the fixed frame O_F. The term $\boldsymbol{\alpha}_B$ x **r** can be described as tangential acceleration and $\boldsymbol{\omega}_B$x($\boldsymbol{\omega}_B$x**r**) is the centripetal acceleration in a rigid node motion.

Table I - The characteristics of simulated earthquakes.

	Total Time (sec)	**ΔT_{max} (sec)**	**ΔT_{min} (sec)**	**Number of oscillations**	**Maximum Frequency (Hz)**
Earthquake Type 1	45	2.0	0.8	30	1.2
Earthquake Type 2	50	2.0	1.5	30	0.8

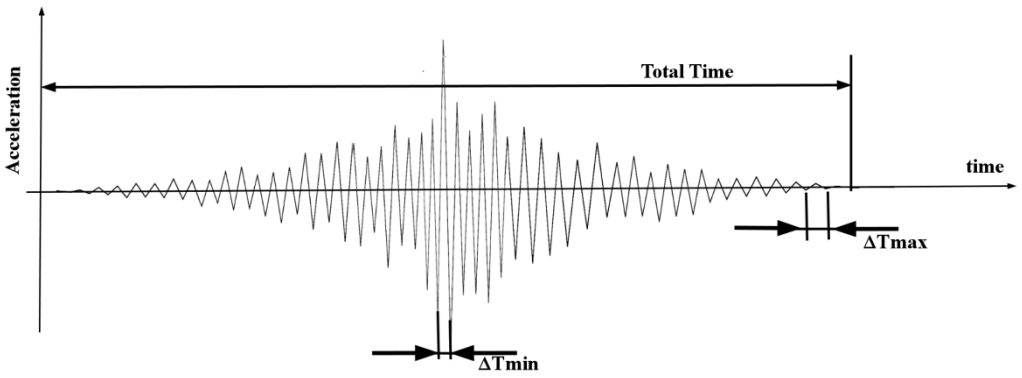

Figure 6 Main characteristics of simulated reference earthquake.

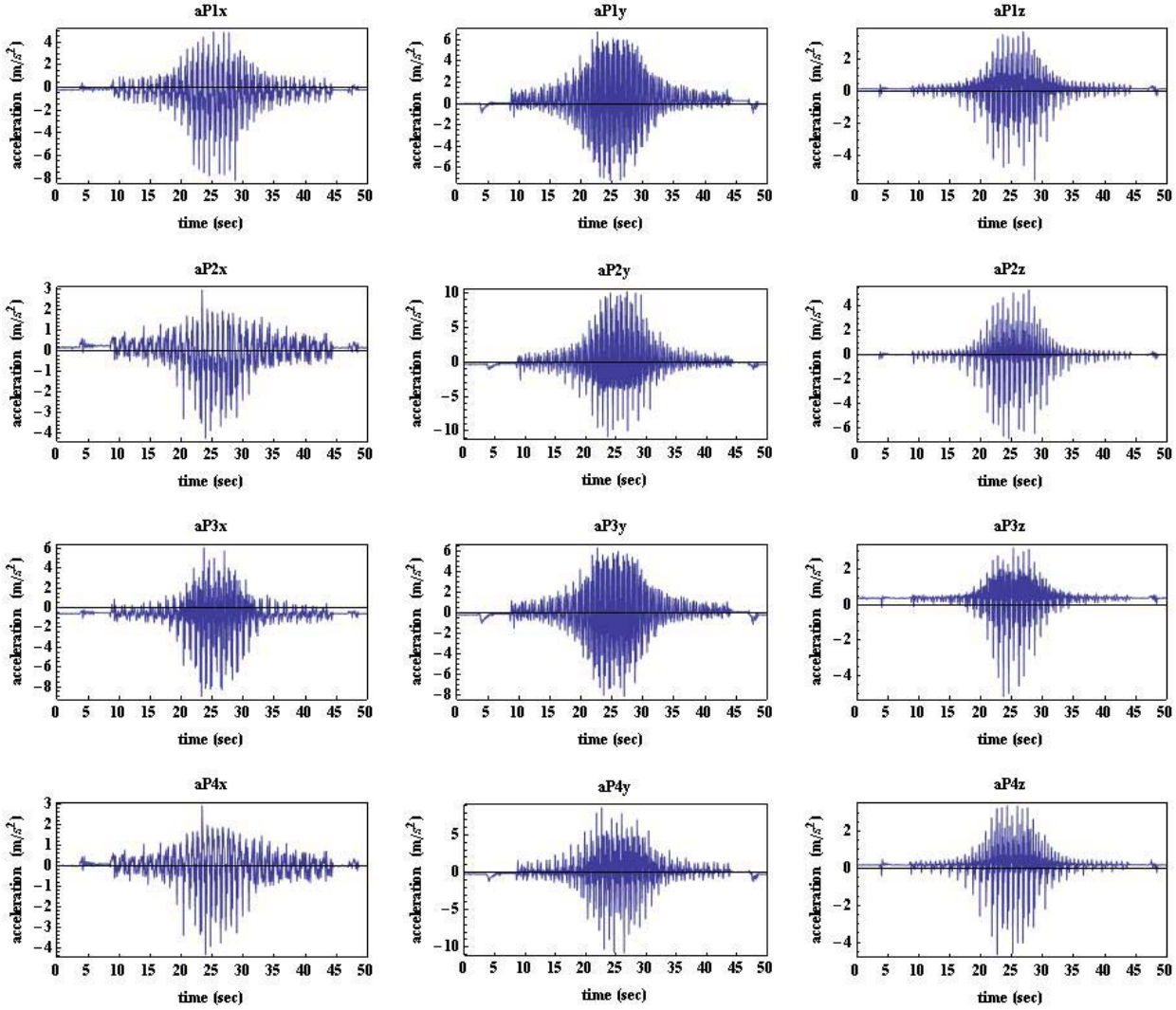

Figure 7 Measured acceleration data during an earthquake simulation as acquired from the accelerometers in the set up of Figure 4.

In order to calculate the acceleration as measured by a sensor that is attached at position $\mathbf{r}$ in the body frame O_B the sensitivity axis $\mathbf{s}$ and the sensors' metrological signal offset $\mathbf{a}_0$ must considered in Eq.(2) to give

$$\mathbf{a}_S = \mathbf{s}^T \left(\mathbf{a}_B + \boldsymbol{\alpha}_B \times \mathbf{r} + \boldsymbol{\omega}_B \times (\boldsymbol{\omega}_B \times \mathbf{r}) \right) + \mathbf{a}_0 \tag{3}$$

Equation (3) can be written in vector form as

$$\mathbf{a}_S = \mathbf{c}\,\mathbf{z} + \mathbf{a}_0 \tag{4}$$

where the vector can be expressed as

$$\mathbf{c} = \left[s_x, s_y, s_z, s_z r_y - s_y r_z, s_x r_z - s_z r_x, s_y r_x - s_x r_y, -(s_y r_y + s_z r_z), \right.$$
$$\left. -(s_x r_x + s_z r_z), -(s_x r_x + s_y r_y), s_x r_y + s_y r_x, s_x r_z + s_z r_x, s_y r_z + s_z r_y \right]^T$$

$$\mathbf{z} = \left[a_{B,x}, a_{B,y}, a_{B,z}, \alpha_{B,x}, \alpha_{B,y}, \alpha_{B,z}, \right.$$
$$\left. \omega_{B,x}^2, \omega_{B,y}^2, \omega_{B,z}^2, \omega_{B,x}\omega_{B,y}, \omega_{B,x}\omega_{B,z}, \omega_{B,y}\omega_{B,z} \right]^T$$

By using four sensors with twelve sensitive axes it is possible to directly compute $\boldsymbol{\alpha}_B$ as well as $\mathbf{a}_B$ and $\boldsymbol{\omega}_B$. In fact, the problem becomes as linear system that can be written in vector form as

$$\mathbf{y} = \mathrm{A}\,\mathbf{z} + \mathbf{a}_{0,S} \tag{5}$$

with $\mathbf{y} = \left[\mathbf{a}_{S1}, \mathbf{a}_{S2}, \cdots, \mathbf{a}_{S12} \right]^T$, $\mathrm{A} = \left[\mathbf{c}_{S1}, \mathbf{c}_{S2}, \cdots, \mathbf{c}_{S12} \right]^T$ and $\mathbf{a}_{0,S} = \left[\mathbf{a}_{0,S1}, \mathbf{a}_{0,S2}, \cdots, \mathbf{a}_{0,S12} \right]^T$.

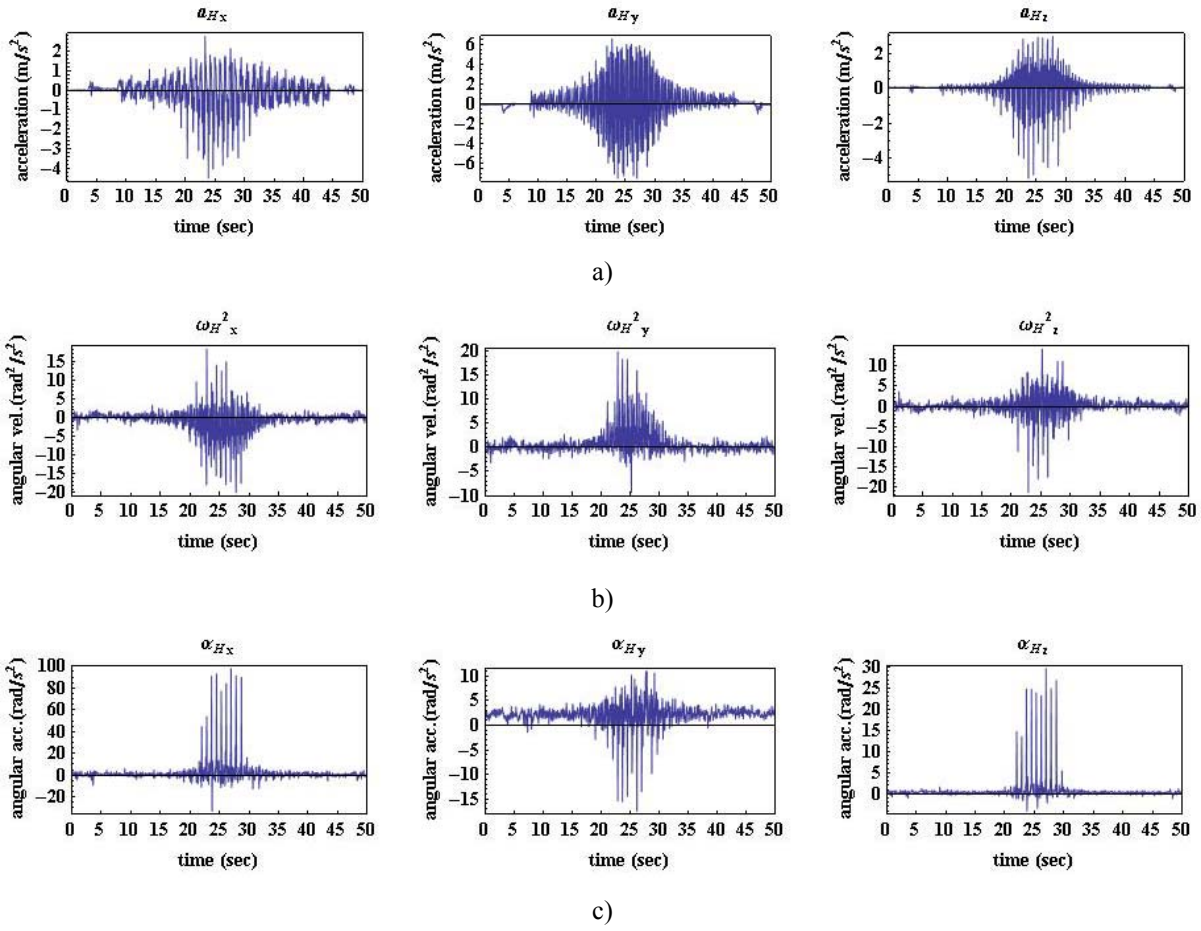

Figure 8 An example of calculated data during an earthquake simulation:
a) acceleration of the platform center H, b) square angular platform velocity, c) angular platform acceleration.

By inverting A it is possible to calculate characteristics of vector **z** of the relative body motion as function of a measured vector **y** by the expression

$$\mathbf{z} = \mathrm{A}^{-1}\left(\mathbf{y} - \mathbf{a}_{0,\mathrm{S}}\right) \tag{6}$$

By using Eq. (6) the linear acceleration $\mathbf{a}_{\mathrm{H}}$, angular acceleration $\boldsymbol{\alpha}_{\mathrm{H}}$, and angular velocity $\boldsymbol{\omega}_{\mathrm{B}}$ can straightforward calculated. An example is reported in Fig. 8 as referring to a simulated earthquake.

5 EXPERIMENTAL SET-UP WITH MECHANISM MODELS AND TEST RESULTS

Experimental tests have been carried out by using a slider-crank linkage with servo motor, a small car model, and LARM Hand as test-bed mechanisms that are sensored with acceleration or force sensors. Maximum acceleration values of the center point H can be used to summarize the earthquake disturbance of the platform motion. Maximum accelerations for the used earthquakes of type 1 and type 2 in performed tests are $a_{h1,max} = 8.4$ m/s^2 and $a_{h2,max} = 5.29$m/s^2, respectively. Experimental data from mechanism sensors during earthquake disturbance are discussed specifically in the next sub-sections for each tested mechanism.

5.1 SLIDER CRANK ACTUATED BY SERVO MOTOR

In Fig. 10a) an accelerometer is shown attached to the slider sensing axis and a torque sensor is used to monitor torque evolution during operation. In Fig. 11.a) and b) plots of torque of the motor and acceleration of the slider are shown for the case without earthquake disturbance when crank rotates at 90 rpm and 180 rpm, respectively. It can be noted that there is a noisy measurements that are very likely caused by backlash of the components assembly and manufacturing tolerances.
In Fig. 12.a) and b) experimental measures of motor torque and slider acceleration are plotted during earthquake disturbance when crank rotates at 90 rpm and 180 rpm, respectively.

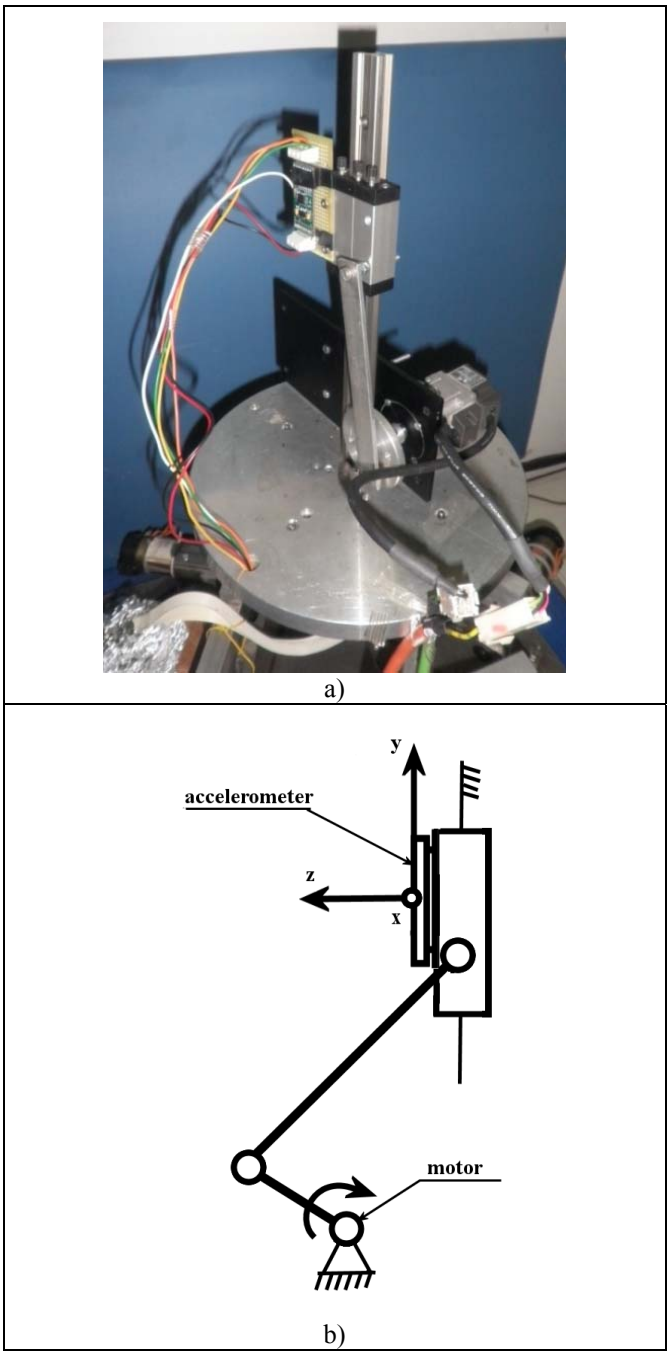

Figure 10 A test-bed slider-crank mechanism with a servo motor: a) an experimental set up with accelerometer on the slider; b) sensing axis of the accelerometer.

It can be noted from acceleration measures of slider in Fig. 12 and in Table II that not only the shape and amplitude of the acceleration of the slider is strongly modified during the simulated earthquakes are but even the oscillations of the slider are almost completely vanished. The torque of the motor shows relatively significant disturbs in amplitude and the shape and oscillation look very similar to the operation in the case of stationary frame with no earthquake.

5.2 LARM HAND

The LARM Hand prototype has been used in this work as test-bed mechanism as a case of study of robotic systems. The LARM Hand in Fig. 13 is composed of three fingers with the aim of performing a human-like grasping by each finger with one DoF motion by using a suitable mechanism [18]. The peculiarity of the finger mechanism design consists in a cross four-bar linkage that during the finger motion remains within the finger body.

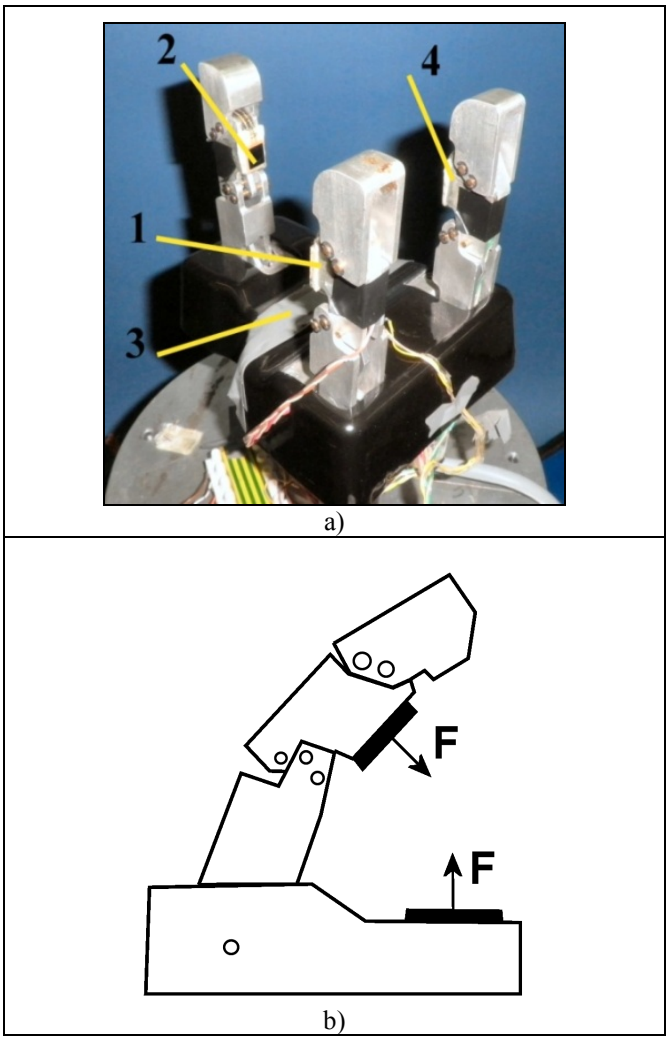

Figure 13 LARM Hand: a) a prototype, b) sensor locations.

Because the linkage design and its one DOF mobility for the finger mechanisms, a grasp can be regulated through a fairly simple control by using force sensor signals and an industrial small PLC for operation. The LARM Hand can be used as a grasping end-effector in robots and automatic systems. Each finger of LARM Hand has 3 joints and 1 actuator. The range of motion for the prototype in Fig. 13 is 40 degree for finger inputs and 140 degree for fingertip links. The used LARM Hand prototype is equipped with 4 force sensors whose range of sensitivities is from 1 to 100 N with a resolution lower than 0.5% of its full scale. The

dimensions of the finger are 1:1.2 of the human finger size and the hand has a volume of 110x240x120 mm where as the size of objects that can be grasped is between 10 to 100 mm. Both types of earthquakes have been tested with LARM Hand during grasping a cylinder block. Results are summarized in Table III for test outputs like the example in Fig. 14.

Table III lists typical forces acting on a tested object during static conditions and during earthquake disturbances. Fig. 14 show plots of forces on gripper fingers and palm with an oscillatory evolution during the earthquake disturbance with a considerable change at the end. These results show clearly that an earthquake strongly affects characteristics of robotic operation such as output force, repeatability of the operation in frequency and efficiency, and reliability of the action in term also of precision accuracy. For the LARM Hand the grasping force efficiency by the fingers can decrease during an earthquake and it can happen the slipping of a grasped object within the fingers. In addition, the applied force to the object can increase at the end of the disturbance and therefore, the object can be even damaged.

5.3 VEHICLE MODEL

Comfort and safety in transportation vehicles is felt by human users mainly in terms of acceleration of the vehicle. Motion and force characteristics describe these properties in vehicles during the run. In general, those characteristics are analyzed under any disturbance which can produce uncomfortable or unsafe operation. But even an earthquake can produce significant risk disturbance both for comfort and safety in vehicle functioning.

For this work a specific vehicle model is designed for characterizing earthquake effects on vehicle operation. The used scaled vehicle model in Fig. 15a) is equipped with a dc motor and installed on a rail. A force sensor and a three axis accelerometer are attached on the vehicle as shown in Fig. 15b). The running of the vehicle is simulated by letting the motor giving the wheel rotation. Due to friction on the wheels from the rail when voltage is applied to dc motor a force is applied on the force sensor as measure of the motion action.

Figure 17 shows plots of pushing force F for test with car model under earthquake disturbance. Comparing those plots with static data shown in Fig.16 it can be noted a relevant change in the car behaviour with significant oscillations.

Details of these changes can be appreciated in Fig. 18 with zoomed views of force data between 20 to 25 seconds of earthquake motion when the seismic accelerations are at maximum. Considering the different voltages applied to motor of the mechanism as reported in Figs. 17 and 18 with the values in Table IV earthquake disturbance seems to affect the car operation in the same way so that change in the wheel action will not help in reducing the disturbs.

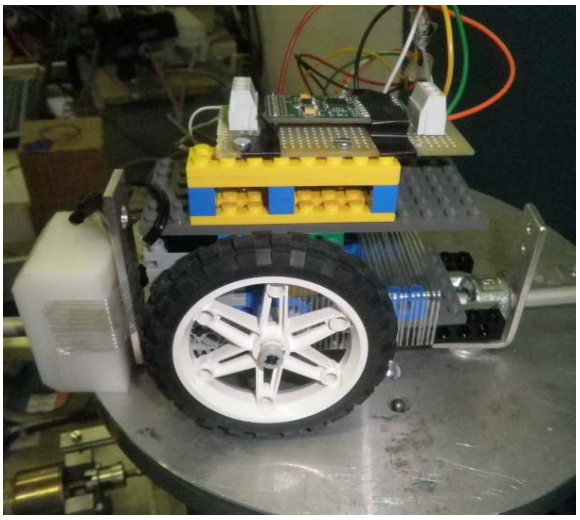

Figure 15 The used scaled car model with force and accelerometer sensors: a) an experimental setup with a LEGO prototype; b) sensors and directions.

Table II - Summary of test results with slider-crank mechanism.

Test measure - Test conditions	**Test data (earthquake frequency – crank rotation speed)**	**Earthquake type 1**	**Earthquake type 2**	**Stationary**
$ay_{max}(m/s^2)$ slider crank mechanism	15kH-90rpm	7.530	4.15	2.508
	30kH-180rpm	11.64	10.81	8.211
	60kH-360 rpm	16.90	16.03	13.97

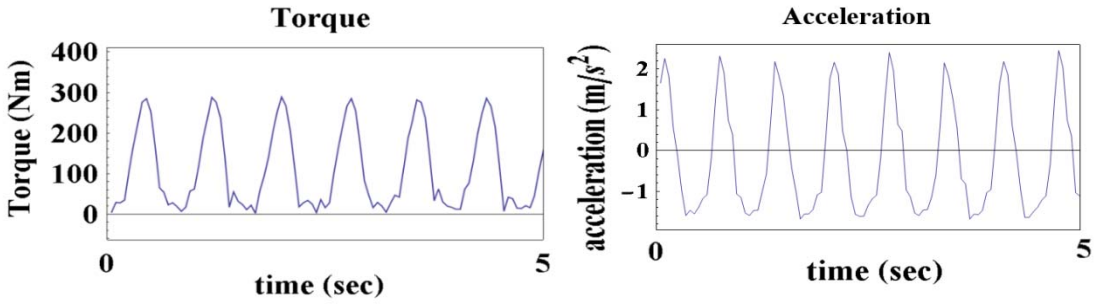

a)

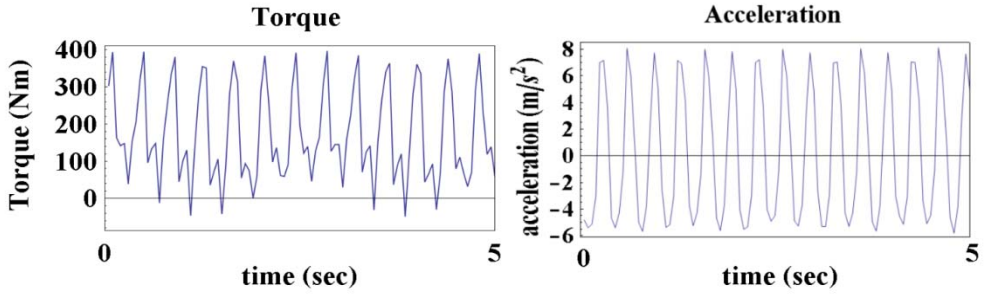

b)

Figure 11 Acquired measurements for a test with slider-crank mechanism in Fig. 10 with no earthquake disturbance: a) torque of the motor and acceleration of the slider with crank rotation 90 rpm; b) torque of the motor and acceleration of the slider with crank rotation 180 rpm.

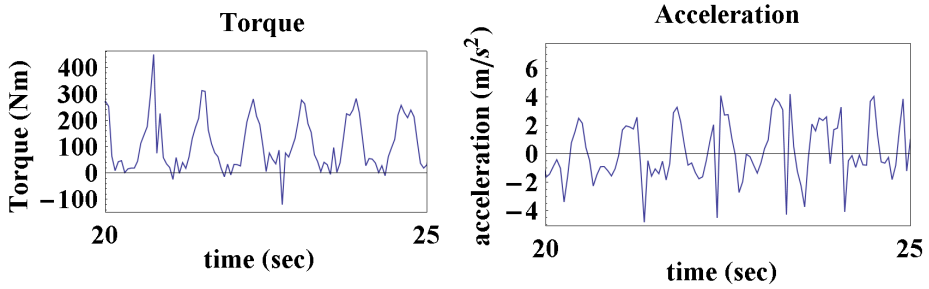

a)

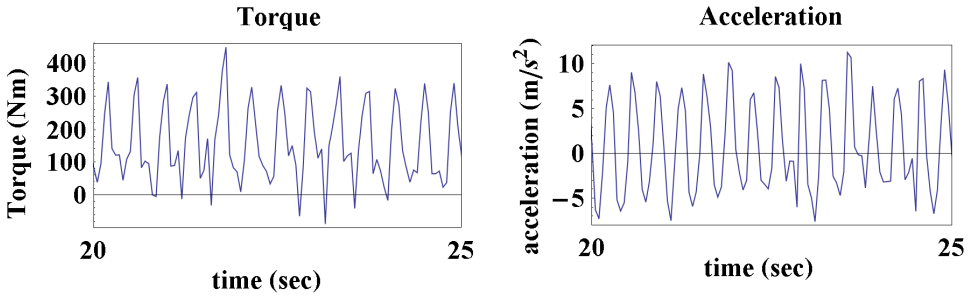

b)

Figure 12 Acquired measurements for a test with slider-crank mechanism in Fig. 10 with earthquake disturbance of type in Table I: a) torque of the motor and acceleration of the slider with crank rotating at 90 rpm, b) torque of the motor and acceleration of the slider with crank rotating at 180 rpm.

Table III - Summary of test results as grasping forces by LARM Hand.

Test measures - Test conditions	Force range	Earthquake type 1	Earthquake type 2	Stationary
Forces F1, F2, F3 and F4 in LARM Hand (N)	Max	2.65, 2.65, 2.53, 2.99	2.23, 2.30, 2.37, 3.10	2.52, 2.57, 2.47, 2.97
	Min	1.9, 1.99, 1.91, 2.25	1.64, 1.73, 1.77, 2.33	1.89, 1.94, 1.86, 2.23

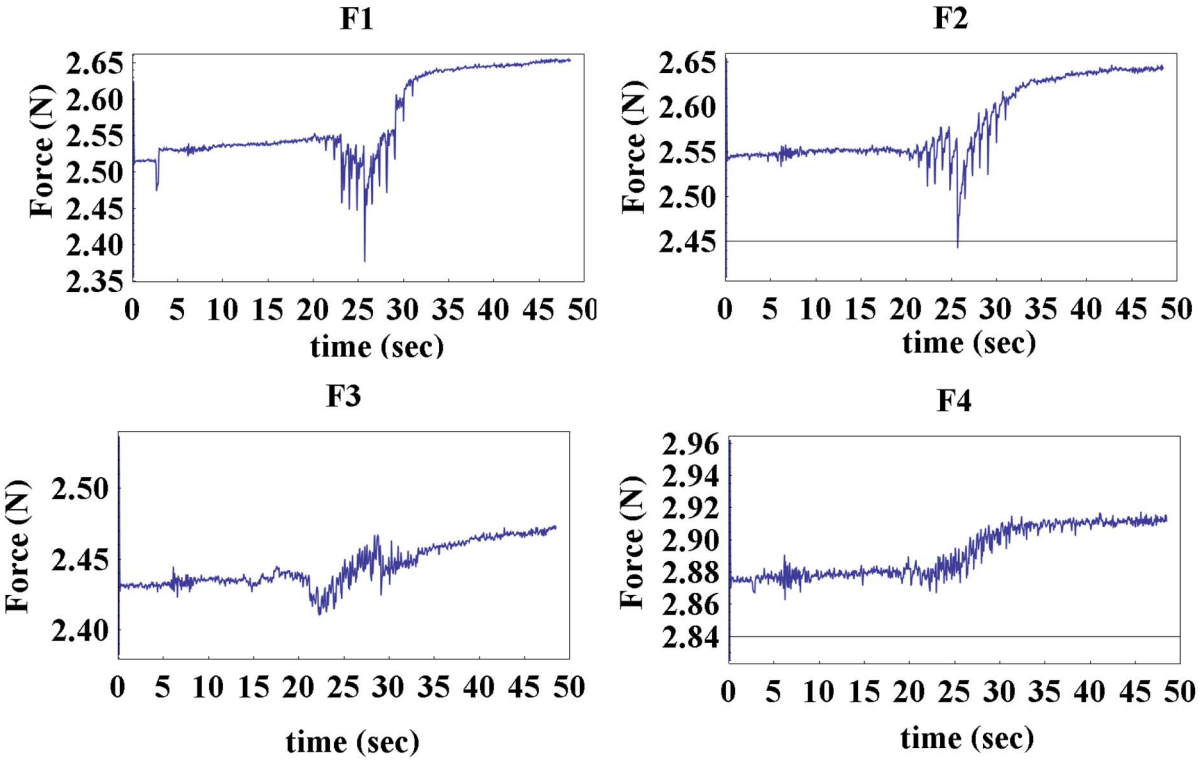

Figure 14 Acquired force measurements for a test with LARM Hand in Fig. 13 with earthquake disturbance of type 1.

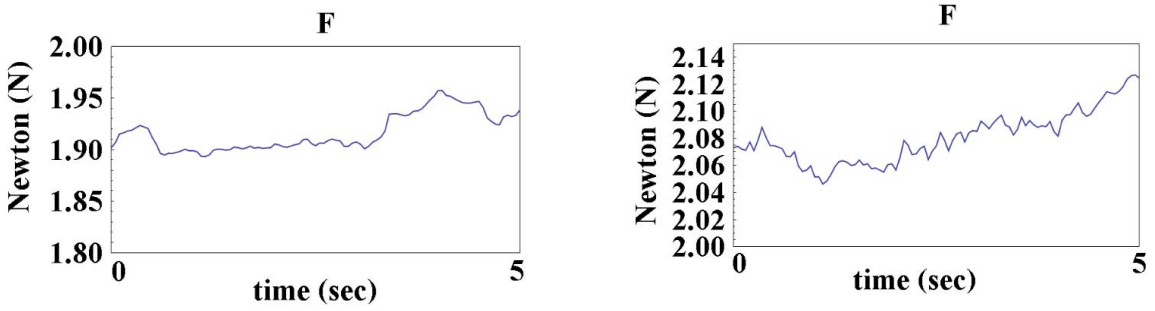

a) b)

Figure 16 Acquired measurements of pushing force F for a test with car model in Fig.15 without earthquake disturbance: a) with applied voltage of 7V; b) with applied voltage of 9V.

Table IV - Summary of test results of pushing forces by scaled car.

Test measures - Test conditions	Force range vs input voltage		Earthquake type 1	Earthquake type 2	Stationary
Pushing force (N)	7v	Max	2.086	2.121	1.980
		Min	1.189	1.604	1.839
	9v	Max	2.102	2.091	1.995
		Min	1.155	0.012	1.95

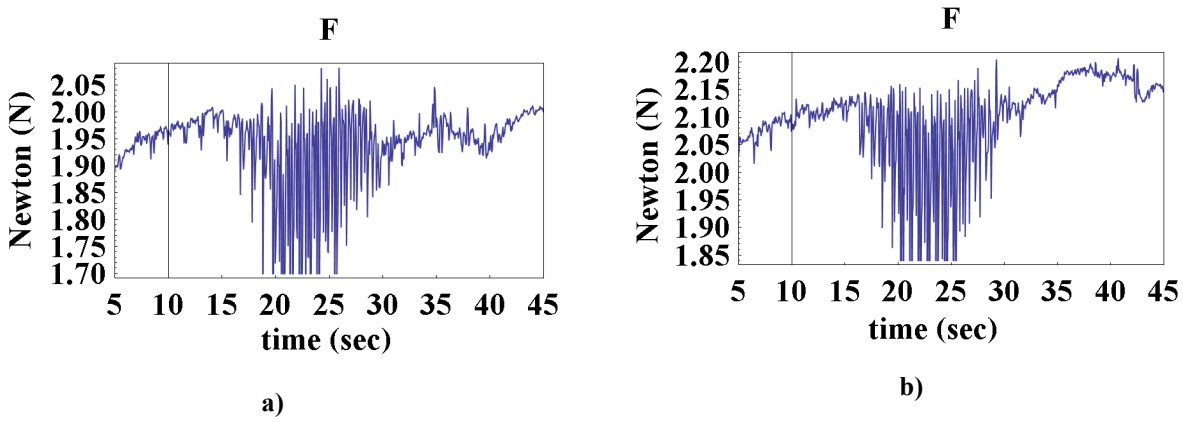

Figure 17 Acquired measurements of pushing force F for a test with car model in Fig.15 with earthquake disturbance: a) with applied voltage of 7V; b)with applied voltage of 9V.

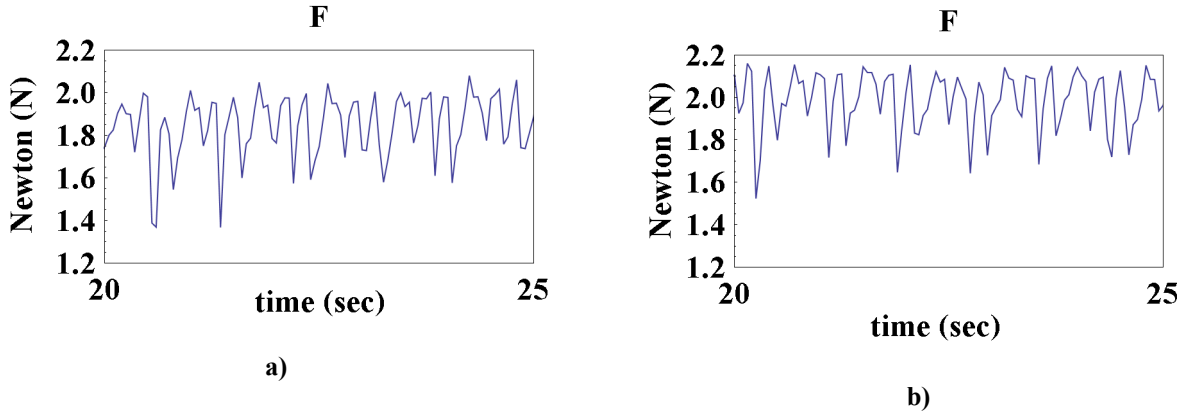

Figure 18 Zoomed views of the acquired measurements of pushing force F for a test with car model in Fig.17: a) with applied voltage of 7V; b)with applied voltage of 9V.

6 CONCLUSIONS

In this work earthquake influence on machinery operation has been investigated by an analysis and reproduction of earthquake motion with the help of CaPaMan. The sensitivity of the operation characteristics of machinery to earthquake disturbance can be characterized in terms of acceleration response and force of the output of machinery operation. Experimental tests have been carried out by using a slider-crank linkage with DC and servo motors, a scaled car model, and LARM Hand as test-bed mechanisms with proper acceleration or force sensors. The results show that an earthquake will strongly affect the acceleration of the mechanism operation both in shape and amplitude of the output motion. Task force of a mechanism affected during earthquake and it is observed that it is left increased after earthquake disturbance.

The results of laboratory experiments on a slider-crank linkage and a vehicle model shows that earthquake disturbance strongly affects the operation of a vehicle such as a train. Therefore increasing speed or force of the input of the vehicle will decrease the effects of unexpected seismic disturbance. Thus, a train operating under an earthquake disturbance should not brake but very likely it should increase the speed.

REFERENCES

[1] J.P. Conte, T.L. Trombetti, Linear dynamic modeling of a uni-axial servo-hydraulic shaking table system. Earthquake Engineering and Structural Dynamics 29 (2000) 1375-1404.

[2] J.L. Kuehn ,D.S. Epp, W.N. Patten, A high fidelity control for seismic shake tables. Proc. 12th Engineering Mechanics Conference, 17–20 May, LaJolla, CA.,1998, pp. 783–786.

[3] A.J. Crewe, R.T. Severn, The European collaborative program on evaluating the performance of shaking tables, Phil. Trans. RoyalSoc. London, Series A, 359-1786, 2001, pp. 1671-1696.

[4] N. Ogawa, K. Ohtani,T. Katayama, H. Shibata, Construction of a three-dimensional large scale shaking table and development of core technology, Phil. Trans. Royal Soc. London, Series A, 359-1786, 2001, pp. 1725-1751.

[5] J.S. Shortreed, F. Seible, A. Filiatrault, G. Benzoni, Characterization and testing of the Caltrans Seismic Response Modification Device Test System. Phil. Trans. Royal Soc. London, Series A359-1786, 2001, pp. 1829-1850.

[6] W.F. Chen, C. Scawthorn, Earthquake engineering hand book, CRC Press, Boca Raton, 2003.

[7] M. Bruneau, A. Reinhorn, M. Constantinou, S.T. Thevanayagam, A. Whittaker, S.Y. Chu, M. Pitman, K. Winter, Versatile shake tables and large-scale high-performance testing facility towards real-time hybrid seismic testing, Proceedings of ASCE Structures Congress, Denver April, 2002.

[8] M. Ceccarelli, F. Pugliese, C. Lanni, J.C.M. Carvalho, CaPaMan (Cassino Parallel Manipulator) as sensored earthquake simulator. Proceedings of the 1999 IEEE/RSJ International Conference on Intelligent Robots and Systems, Kyongiu, 1999, pp. 1501-1506.

[9] E. Ottaviano, M. Ceccarelli, Application of a 3- DOF parallel manipulator for earthquake simulations, IEEE Transactions on Mechatronics 11-2, 2006, pp. 140-146.

[10] J.C.M. Carvalho, M. Ceccarelli. Seismic motion simulation based on CaPaMan simulation, Journal of the Brazilian Society of Mechanical Sciences, 25-3, 2002, pp. 213-219.

[11] M. Ceccarelli., E. Ottaviano, C. Florea, T.P. Itul, A. Pisla, An experimental characterization of earthquake effects on mechanism operation, IEEE-TTTC International Conference on Automation, Quality and testing, Robotics, AQTR 2008,Cluj-Napoca, 2008.

[12] O. Selvi, M. Ceccarelli, Interpretation of Earthquake Effects on Mechanism Operation: An Experimental Approach, Journal of Naval Science and Engineering, 8-2, 2012, pp. 31-45.

[13] W.F. Chen, C. Scawthorn, Earthquake Engineering Handbook, CRC Press, Boca Raton, 2003.

[14] IFToMM 2003, special issue 'Standardization and Terminology', Mechanism and Machine Theory, Vol.38, n.7-10.

[15] J.J. Uicker, G.R. Pennock, J.E. Shigley, Theory of Machines and Mechanisms, Oxford University Press, Oxford, 2003.

[16] Lopez-Cajùn C.S., Ceccarelli M., Mecanismos: Fundamentos cinematicos para el diseno y la optimizacion de la maquinaria, Trillas, Ciudad de Mexico, 2008 (ISBN 978-968-24-8181-9); 2nd Edition 2014.

[17] B. Zappa, G. Legnani, A. J. van den Bogert, R. Adamin, On the Number and Placement of Accelerometers for Angular Velocity and Acceleration Determination, Journal of Dynamic Systems, Measurement, and Control, September 2001, Vol. 123, pp. 552-554

[18] G. Carbone, M. Ceccarelli, Design of LARM Hand: problems and solutions, Journal of Control Engineering and Applied Informatics, 10-2, 2008, pp. 39-46.